Simulation of a metamaterial containing cubic high dielectric resonators

Jaewon Kim and Anand Gopinath
Department of Electrical and Computer Engineering, University of Minnesota, 200 Union Street SE, Minneapolis, Minnesota 55455, USA
(Received 22 October 2006; revised manuscript received 12 August 2007; published 24 September 2007)

Simulation results of a metamaterial structure which uses cubic high dielectric resonators, periodically embedded in a low dielectric background in a cubic lattice, are presented. Cubic dielectric resonators have degenerate modes, which imply that the TE and TM modes have the same resonant frequency. The proposed metamaterial shows the negative refractive index characteristics around the resonance frequency of the cubic resonators, and since no plasmonic components are involved, the losses are expected to be low.

DOI: 10.1103/PhysRevB.76.115126 PACS number(s): 78.20.Ci, 41.20.Jb, 42.25.Bs

I. INTRODUCTION

Metamaterials were initially discussed by Veselago in 1968,[1] and subsequently by Pendry,[2] and have negative permittivity (ε_r) and negative permeability (μ_r) simultaneously over a fixed frequency range, and therefore are also called negative refractive index (NRI) materials or double-negative (DNG) materials. A structure comprising of split ring resonators (SRRs), proposed by Pendry *et al.*,[3] with additional metal lines, printed on substrates was experimentally demonstrated as operating as a negative index material by Shelby and Smith,[4] and subsequently several metamaterial designs have been proposed, both with plasmonic components,[5] and with purely dielectric components.[6–8]

Negative index materials require an electric dipole or quadrupole resonance, and, simultaneously at the same frequency, a magnetic dipole or quadrupole resonance. With plasmonic components such simultaneous resonances have been designed with considerable ingenuity.[5] However, with purely dielectric designs, a Mie resonance of the dielectric particle obtains one type of resonance, and the other resonance is obtained by Bragg scattering and interference, or by other means.[6–8] A recent paper[6] has obtained the quadrupole electric resonance in dielectric rods, and the associated displacement current creates the magnetic resonance at the same frequency to obtain negative index effects. Another paper[7] has a periodic structure composed of two heterogeneous spheres placed side by side as the basic element, one resonant in the TE mode and the other in the TM mode both at the same frequency to obtain the negative index. A third paper suggests a periodic structure with a single sphere with a finite value of μ_r, which gives rise to the negative refractive index.[8]

In this paper, we propose a metamaterial with cubic high dielectric resonators (CHDRs) in a cubic lattice embedded in a low dielectric background. The cubic high dielectric resonator has degenerate TE and TM resonant modes, and the combination of the Mie resonances of the cube and the Bragg scattering and interference[9,10] leads to negative index. For the higher order Mie resonances, two possibilities arise, one in which the displacement electric or magnetic current causes the second resonance to appear,[6] or both resonances appear due to the degeneracy of the modes of the cube. These will be discussed in a subsequent paper.

In this paper, the scattering parameter approach obtains the permittivity and permeability of the composite structure. The cubic resonator periodic structure is simulated using a three-dimensional (3D) electromagnetic (EM) simulation program to obtain the scattering parameters (S parameters), and from these, the effective values of permittivity (ε_r), permeability (μ_r), and index are calculated. In this paper, the calculation of the modes of the isolated cubic resonator are first discussed followed by band structure calculations of the cubic resonators in a lattice structure, and finally the scattering parameter calculations to obtain the permittivity, permeability, and index of this lattice structure are outlined.

II. SIMULATION OF PROPOSED METAMATERIAL STRUCTURE

The properties of the proposed structure were obtained using two types of numerical simulations, the first is the finite difference time domain (FDTD) simulation to obtain the wave-vector band structure of the proposed CHDR lattice structure, and the second is the finite element simulation for the S parameters also of the proposed CHDR lattice structure, to obtain the constitutive effective parameters. Theoretically, a rectangular cavity resonator with metal walls has the resonant frequencies given by[11]

$$f_{mnp} = \frac{1}{2\sqrt{\varepsilon\mu}}\sqrt{\left(\frac{m}{W}\right)^2 + \left(\frac{n}{H}\right)^2 + \left(\frac{p}{L}\right)^2}, \qquad (1)$$

where integers m,n, and p denote the number of half wave variations in the x,y, and z directions, respectively, and

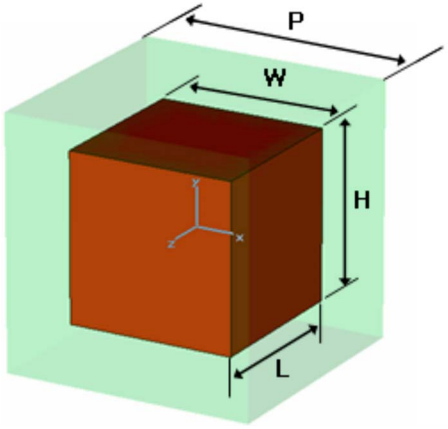

FIG. 1. (Color online) Unit cell of the CHDR structure used in the numerical simulation, side $W=,H=,L=8$ mm, spacing $P=12$ mm, inner cube $\varepsilon_r=40$, and outer cube $\varepsilon_r=2.08$.

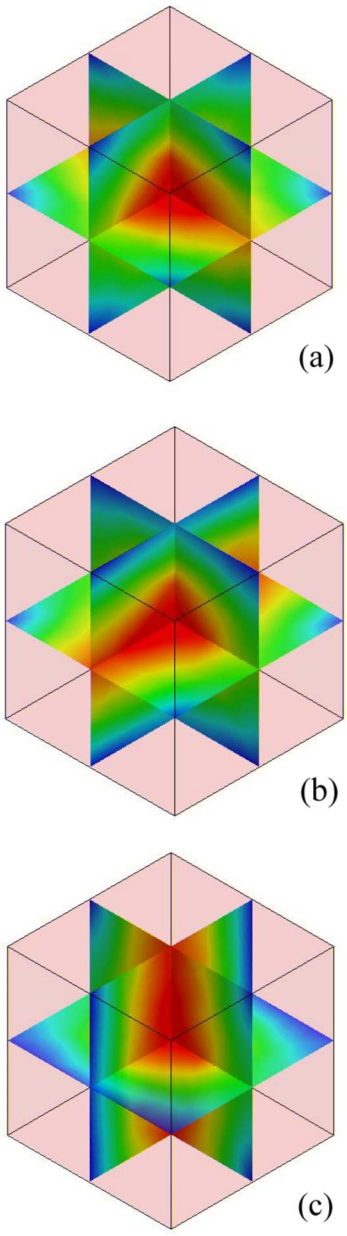

FIG. 2. (Color online) Magnetic field distributions of three lowest-order modes for the CHDR structure (a) mode 1, (b) mode 2, and (c) mode 3.

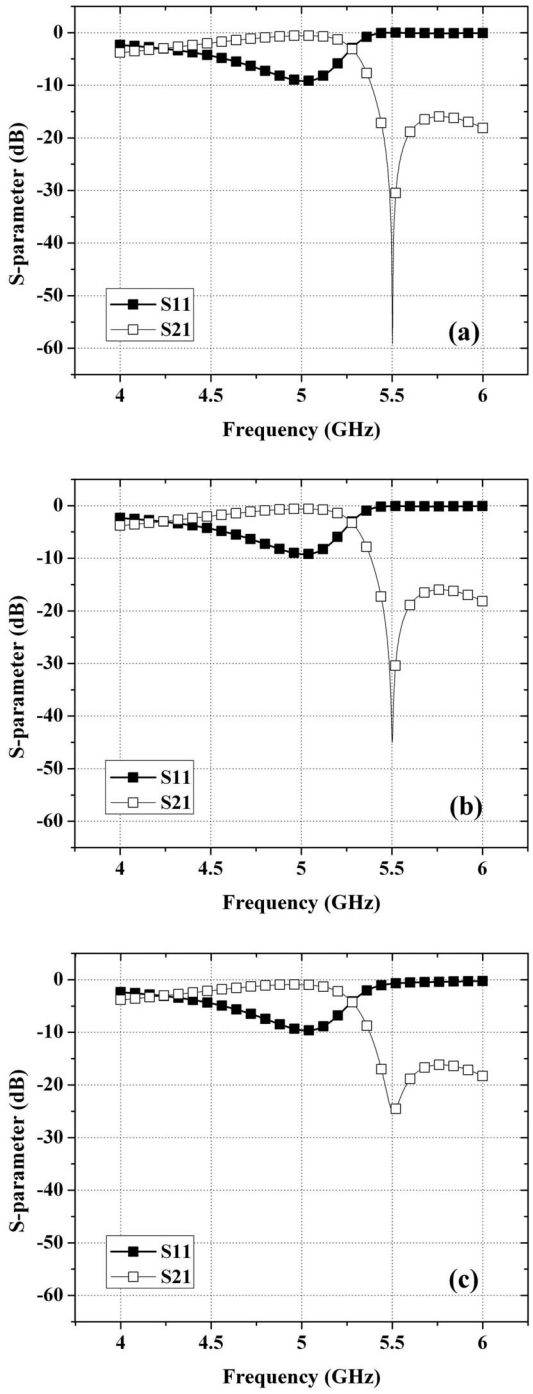

FIG. 3. S parameter and effective constitutive parameters for the (a) lossless case tan δ=0, the lossy cases (b) tan δ=0.001, and (c) tan δ=0.01.

W,H, and L denote the x,y, and z dimensions of the rectangular cavity, respectively. For a cubic cavity resonator, all sides are equal in length, which implies that $W=H=L$, and all the lowest-order modes are degenerate. For example, TM110, TE011, and TE101 have the same field patterns in the case of an air filled cubic cavity resonator. The resonant frequency of these degenerate modes is

$$f_{\text{deg}} = \frac{1}{\sqrt{2}\sqrt{\varepsilon\mu}\cdot W}. \tag{2}$$

With a high dielectric resonator, boundary conditions at the walls may be approximated to be open circuits,[12] and in this case, the resonant frequencies of the modes are also given by Eqs. (1) and (2). The unit cell of CHDR structure used in the numerical simulations has a low dielectric background, ε_r =2.08, with the cubic high dielectric resonator, ε_r=40, as shown in Fig. 1.

According to the eigenmode simulation, this unit cell of the CHDR structure with perfect magnetic boundaries has TE and TM degenerate modes at 4.186 GHz. This is close to the degenerate frequency, 4.192 GHz, calculated from Eq. (2). Figure 2 shows the magnetic field distributions of three

TABLE I. The calculated quality factor (Q) of CHDR structures.

Loss tangent (δ)	Quality factor (Q)
0 (lossless)	18000
0.0001	6500
0.001	1000
0.01	107

lowest-order modes for the CHDR structure. As expected, TE and TM degenerate modes at the same resonant frequency have the same field distributions, but with the axes changed. The quality factor (Q) for CHDR structure is also calculated in Table I for different values of the loss tangent ($\tan\delta$). The 8-mm-size CHDR structure (ε_r=40) embedded in a low dielectric background (ε_r=2.08) was used in all these simulations. With open boundaries, a considerable reduction of the resonator Q occurs, however, in Fig. 3 it is shown, by simulations, that the negative refractive index region of CHDR metamaterial was not changed while its quality factor (Q) was changed by various dielectric loss tangent values as shown in Table I. Both lossless and lossy cases were calculated with $\tan\delta$ varied from 0 to 0.01 in Fig. 3. The method used in these simulations will be introduced in detail in the following sections. Commercial CHDRs claim to have the quality factor(Q) of 2500. When metal plates are placed at top and bottom of CHDR, the radiation loss can be reduced and therefore the higher Q of CHDR can be obtained. This means the CHDR metamaterial in this paper not including any metal plate may have Q less than 100. Since the S-parameter method of calculating the constituent parameters does not allow radiation loss, all simulations in this paper were performed considering the dielectric loss with $\tan\delta$ of 0.01, with Q values of 107, which in effect allows for the radiation loss.

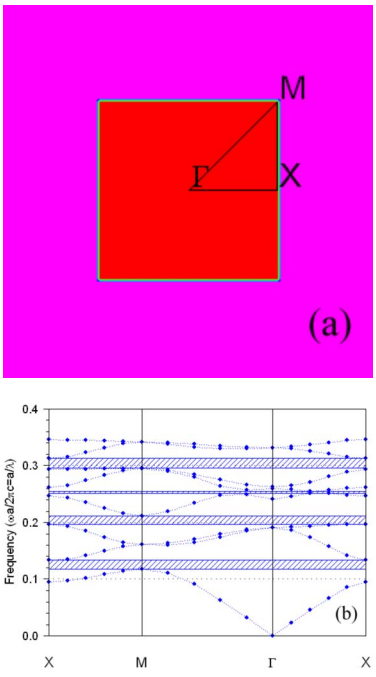

FIG. 4. (Color online) (a) k path and (b) band structure of the CHDR structure for the H (TE) polarization.

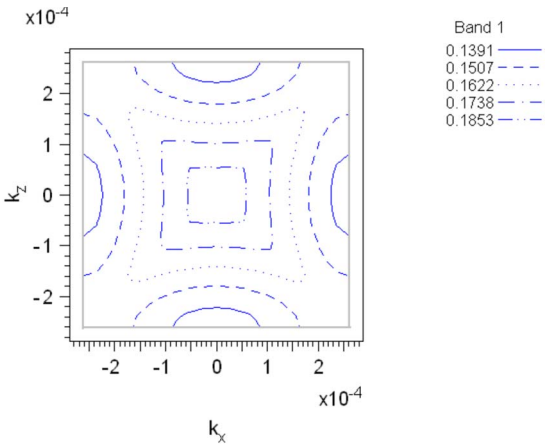

FIG. 5. (Color online) Equifrequency contours of the CHDR structure.

Hatched regions in Fig. 3 are real negative refractive index regions which mean both permittivity and permeability are negative simultaneously.

A. FDTD simulations

A three dimensional (3D) cubic lattice of CHDR unit cells, with lattice spacing a of 12 mm is used in the FDTD simulations to get the band structure and the equifrequency contour for the TE polarization, with the E field in the x-y plane in Fig. 1. The results of this calculation in Fig. 4 show the k path of the structure, and the band diagram of the CHDR structure, with the frequency normalized as $\omega a/2\pi c$, where c is the velocity of light. In Fig. 4(b), the hatched regions are the band gaps for this CHDR structure, and it shows that the negative refractive index region occurs. Figure 5 shows the equifrequency contours of this structure, which are convex in the vicinity of the Γ point. As discussed

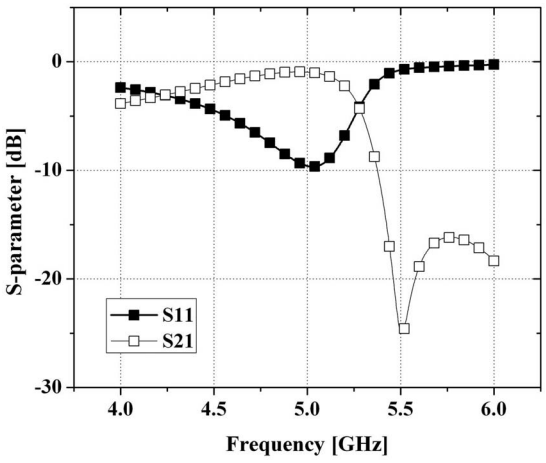

FIG. 6. S-parameter results of a CHDR unit cell.

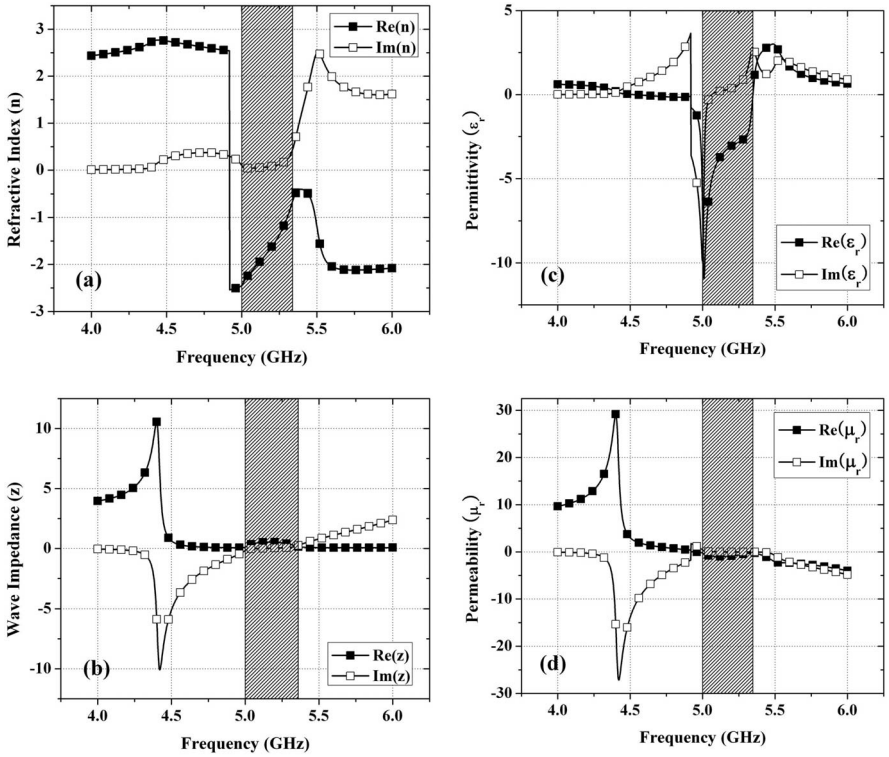

FIG. 7. Effective parameters for a CHDR unit cell (a) refractive index, (b) wave impedance, (c) permittivity, and (d) permeability. Hatched regions are the negative index frequency range.

by Luo,[13,14] frequencies that correspond to all-convex contours have negative refraction confirming the conclusion from Fig. 4(b).

B. Finite element simulations

For the finite element simulations the CHDR unit cell (Fig. 1) is in a cubic lattice, spacing 12 mm, with boundary conditions at the edge of the lattice cell. For the calculations, the direction of propagation of the electromagnetic field is along the z axis, the electric field is oriented along the x axis, and the magnetic field is oriented along the y axis. The calculated results of the S parameter results for a CHDR unit cell are shown in Fig. 6. These results are used in calculating the constitutive effective parameters as discussed below.

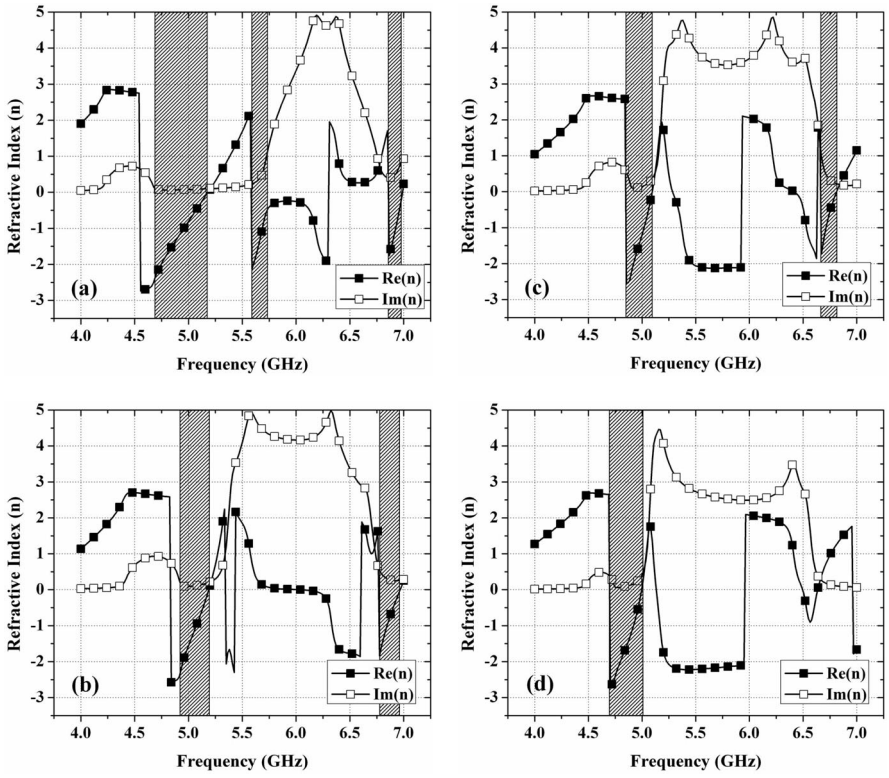

FIG. 8. Refractive index for 3D $3\times3\times3$ CHDRs with a lattice constant (a) $a=10$ mm, (b) $a=12$ mm, (c) $a=14$ mm, and (d) $a=16$ mm. Hatched regions are the negative index frequency range.

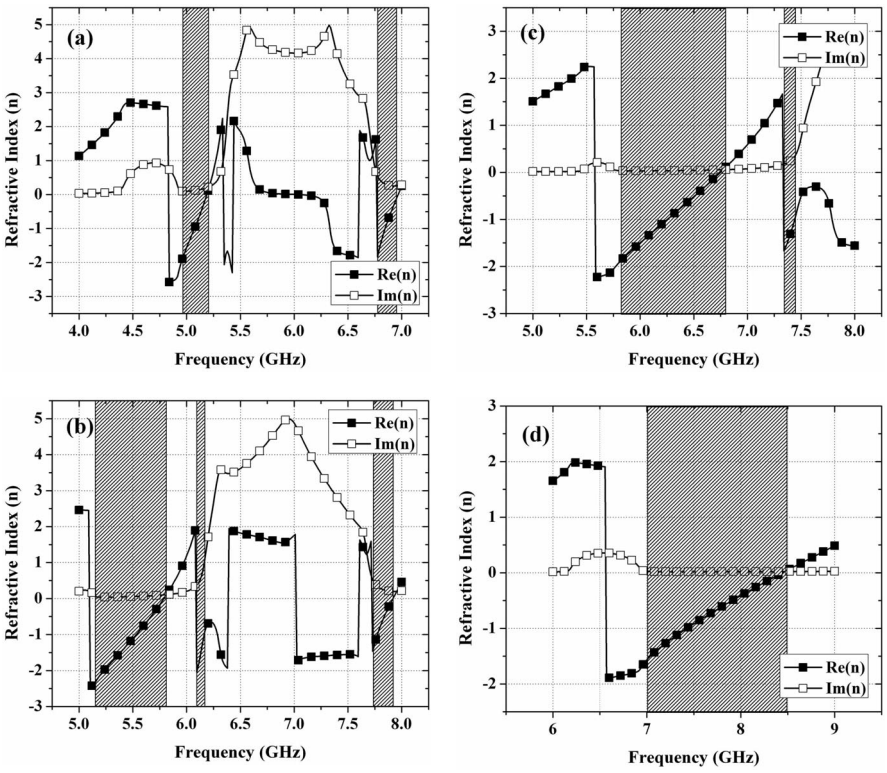

FIG. 9. Refractive index, and constitutive effective parameters with different dielectric constants (a) $\varepsilon_r=40$, (b) $\varepsilon_r=30$, (c) $\varepsilon_r=20$, and (d) $\varepsilon_r=10$. Hatched regions are the negative index frequency range.

C. Retrieving the constitutive effective parameters

The S parameters are related to both the refractive index (n) and the impedance (z). Therefore our retrieval procedure to obtain the refractive index (n) and the wave impedance (z) normalized by the free-space wave impedance $z_0=\sqrt{\mu_0/\varepsilon_0}$ is based on the S parameter results by[15]

$$z = \pm \sqrt{\frac{(1+S_{11})^2 - S_{21}^2}{(1-S_{11})^2 - S_{21}^2}} \tag{3}$$

and

$$e^{ink_0d} = \frac{S_{21}}{1 - S_{11}[(z-1)/(z+1)]}, \tag{4}$$

where n, k_0, and d denote the refractive index, the wave number of the incident wave in a free space, and the thickness of the metamaterial slab, respectively. Once the value of z is obtained from Eq. (3), the value of n is obtained from Eq. (4). However, there is a sign ambiguity in the values of z and n, which is eliminated by imposing the necessary condition for passive materials,[13,16] $\mathrm{Re}(z)\geq 0$ and $\mathrm{Im}(n)\geq 0$. The permittivity (ε_r) and permeability (μ_r) are then directly calculated from $\mu_r=n\cdot z$ and $\varepsilon_r=n/z$. The calculated parameters for a CHDR unit cell are shown in Fig. 7, characterized by permittivity $\varepsilon=\varepsilon'+i\varepsilon''$ and permeability $\mu=\mu'+i\mu''$. The condition $\varepsilon'<0$ and $\mu'<0$ is a sufficient condition for negative refractive index. However, the inequality $\varepsilon''\mu'+\mu''\varepsilon'<0$ is a necessary condition for negative refractive index in a passive medium.[17] Simulations were also performed in a 3D $3\times3\times3$ CHDR structure with a lattice constant (a), varied from 10 to 16 mm, to determine the lattice constant effect. As shown in Fig. 8, simulation results were obtained with the lattice constant varying from 10 to 16 mm in steps of 2 mm. As a result, the negative refractive index region has its bandwidth reduced and then shifts to lower frequency in the lattice constant. The negative refractive indices are negative in 4.8–5 GHz in all cases.

We also consider the effect of dielectric constant of the dielectric resonators in this cubic lattice. All structures in this simulation have the same dimension, the resonator is a cube of 8 mm, and the lattice constant is 12 mm. As shown in Fig. 9, constitutive effective parameters can be controlled by changing the dielectric constant of the resonators. These results show that even when the dielectric constant is as low as 10, the negative index behavior is preserved.

III. CONCLUSIONS

A metamaterial structure has been proposed using cubic high dielectric resonators (CHDRs) which have both TE and TM degenerate modes at the same frequency, and are in a cubic lattice structure, embedded periodically in a low dielectric background. Since no metallic structures are present, there are no conductor losses, but the dielectric losses which are usually small. The proposed CHDR structure has the metamaterial characteristics in a specific frequency range, which can be changed by varying the size of CHDRs, the lattice constant, or the dielectric constant of CHDRs.

[1] V. G. Veselago, Usp. Fiz. Nauk **92**, 517 (1964) [Sov. Phys. Usp. **10**, 509 (1968)].
[2] J. B. Pendry, Phys. Rev. Lett. **85**, 3966 (2000).
[3] J. B. Pendry, J. B. Holden, D. J. Robbins, and W. J. Stewart, IEEE Trans. Microwave Theory Tech. **47**, 2075 (1999).
[4] R. A. Shelby and D. R. Smith, Science **292**, 77 (2001).
[5] R. W. Ziolkowski, IEEE Antennas Propag. Mag. **51**, 1516 (2003); C. G. Parazzoli, R. B. Greeger, K. Li, B. E. C. Koltenbah, and M. Tanielian, Phys. Rev. Lett. **90**, 107401 (2003); A. F. Starr, P. Rye, D. R. Smith, and S. N. Nemat-Nasser, Phys. Rev. B **70**, 113102 (2004); V. M. Shalev, W. Cai, U. K. Chettiar, V. P. Drachev, and A. V. Kildashev, Opt. Lett. **30**, 3356 (2005); G. Dolling, C. Enkrich, M. Wegener, C. M. Soukoulis, and S. Linden, Science **312**, 892 (2006).
[6] Liang Peng, Lixin Ran, Hongshen Chen, Haifei Zhang, Jin au Kong, and Tomas M. Grzegorczyk, Phys. Rev. Lett. **98**, 157403 (2007).
[7] L. Jylha, I. Kolmakov, S. Maslovski, and S. Tretyakov, J. Appl. Phys. **99**, 043102 (2006).
[8] C. L. Holloway, E. F. Keuster, J. Baker-Jarvis, and P. Kabos, IEEE Antennas Propag. Mag. **51**, 2596 (2003).
[9] S. O'Brien and J. B. Pendry, J. Phys.: Condens. Matter **14**, 4035 (2002).
[10] E. Cubukcu, K. Aydin, E. Ozbay, S. Foteinopoulou, and C. M. Soukoulis, Nature (London) **423**, 604 (2003).
[11] D. K. Cheng, *Field and Wave Electromagnetics*, 2nd edition (Addison-Wesley, New York, 1989).
[12] S. Ramo, J. R. Whinnery, and T. Van Duzer, *Fields and Waves in Communication Electronics*, 2nd edition (John Wiley & Sons, New York, 1984).
[13] C. Luo, S. G. Johnson, and J. D. Joannopoulos, Phys. Rev. B **65**, 201104(R) (2002).
[14] C. Luo, S. G. Johnson, and J. D. Joannopoulos, Appl. Phys. Lett. **81**, 13 (2002).
[15] X. Chen, T. M. Grzegorczyk, B. Wu, J. Pacheco, and J. A. Kong, Phys. Rev. E **70**, 016608 (2004).
[16] D. R. Smith and S. Schultz, Phys. Rev. B **65**, 195104 (2002).
[17] R. A. Depine and A. Lakhtakia, Microwave Opt. Technol. Lett. **41**, 315 (2004).